Polarization characteristics of chiral photonic crystal fibers with an elliptical hollow core*

Li She(李 社), Li Jun-Qing(李俊庆)†, and Cao Yu-Sheng(曹雨生)

Department of Physics, Harbin Institute of Technology, Harbin 150001, *China*

(Received 24 April 2013; revised manuscript received 3 August 2013)

The theoretical study of dielectric-chiral photonic crystal fiber (PCF) with an elliptical hollow core is presented. The band structure of chiral photonic crystal (PhC) is calculated by using a modified plane-wave expansion (PWE) method. By examining the out-of-plane photonic bandgaps (PBGs) of chiral PhC, a kind of chiral PCF with a hollow core is designed and their eigenstates are calculated. The distributions of mode field and polarization state are demonstrated, and how the structural asymmetry of the core together with the chirality in the background affects the modal polarization is discussed. The dependences of birefringence on chirality for different ellipticities of core are investigated.

Keywords: chiral medium, photonic crystal fiber with elliptical hollow core, polarization, birefringence

PACS: 78.67.Pt, 42.81.–i, 40.25.Ja, 42.25.Lc **DOI:** 10.1088/1674-1056/22/11/117806

1. Introduction

In recent decades, photonic crystal fibers (PCFs) have attracted a lot of attention from researchers due to their novel optical properties, such as endless single-mode guidance[1,2] and tailorable dispersion,[3] nonlinearity[4–6] and polarization characteristics.[7–9] Generally, there are two types of guiding mechanisms for PCFs. One is the modified total internal reflection, which is usually referred to as index-guiding mechanism and is first realized in experiment;[10] the other is the photonic bandgap (PBG) effect,[11] which leads to confining the light in low-index cores, even in a hollow core. Compared with the former, the latter has some novel characteristics.[12–14] For instance, the PBG effect can be used to design a PCF[12] with flat, near-zero dispersion over a broad wavelength range or a PCF with high anomalous dispersion. Commonly, for a traditional PCF, the linearly polarized modes are supported. However, because of the imperfection in manufacture process, the holes in PCFs cannot be kept perfectly circular during drawing the preform.[2] The nonuniform extrusion or drawing may result in a non-circular symmetry of the core, say the circular core may change into an elliptical one.[15–17] which may cause complicated polarization characteristics. For the fiber communication system, an extremely low degree of birefringence may lead to crucial polarized mode dispersion. Therefore, it is vital to control polarized mode dispersion in the design and fabrication of fibers. The non-circular symmetry of the core may occur on the scale of wavelength, which is called structural asymmetry, while chirality is another asymmetry on a smaller scale, which is named asymmetry of the medium. It is well known that an elliptical core in a PCF with circular-hole background leads to linear birefringence (LB),[15–18] while the chirality of a medium constituting PCF gives rise to circular birefringence (CB),[19,20] which means both of them can be used to design and control dispersion and polarization. When both the elliptical core and chirality exist, some novel features may emerge, especially in polarization.

It should be pointed out that in fact there are two kinds of chiral fibers (including chiral PCF): structurally chiral fiber[20–24] and dielectric-chiral fiber.[19,25–30] In the structurally chiral fiber a helical or twisted structure, whose size is comparable to interested wavelength, is introduced into core or cladding; such a kind of chiral PCF can be used to design circular-polarization-related components, such as the polarization-selective filter[24] and the resonator of angular monumentum.[20] The dielectric-chiral fiber is based on the waveguide structure of an ordinary fiber, in which the constituting medium (such as silica) is partly or entirely replaced by chiral medium. For example, when the chiral molecules are absorbed into the background, the PCF is converted into a chiral one which can be used to design phase retarders and circular polarization maintaining PCF.[19]

To our knowledge, chiral PCFs (with a chiral medium) with an elliptical core have not been reported yet. It is of benefit to the understanding of the interaction of the chirality with the structural asymmetry. In this paper, we will focus on the dielectric-chiral PCF with an elliptical hollow core. Firstly, the band structure of the corresponding chiral photonic crystal (PhC) is calculated with a modified PWE method, the PBGs that are suitable for the optical communication fiber are found, and the effects of chirality on photonic band structure are analyzed. Then, the effect of the ellipticity of the core and that of the chirality of media on polarization distributions of guided modes in chiral PCFs are discussed in detail.

*Project supported by the National Natural Science Foundation of China (Grant No. 60977032).

†Corresponding author. E-mail: jqli@hit.edu.cn

© 2013 Chinese Physical Society and IOP Publishing Ltd

2. Band structure of chiral PhC

A diagram of a PCF that possesses an elliptical hollow core is shown in Fig. 1, in which A and B respectively denote major and minor semi-axes, and chiral cladding contains small air holes of radius r in triangular lattice, whose lattice constant is a.

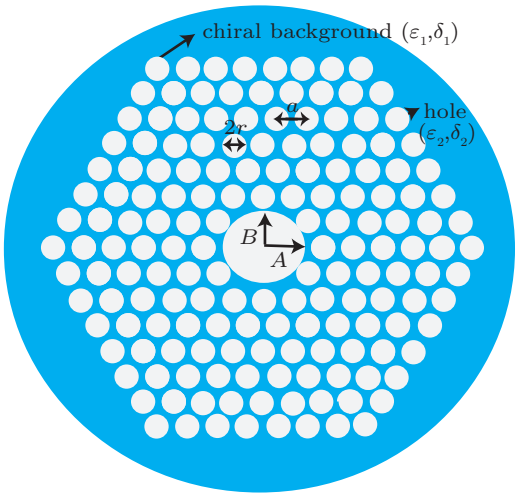


Fig. 1. (color online) Cross section of the chiral PCF, in which the dark background is made of chiral medium, A and B represent the major semi-axis and minor semi-axis in the elliptic core, and a and r denote the lattice constant and radius of the smaller hole, respectively.

In order to study such a PCF, it is necessary to investigate the band structure of the corresponding perfect chiral PhC. To describe the dielectric-chiral medium that fills the background of chiral photonic structure, we adopt the Drude–Born–Fedorov's material equation as constitutive relation, which can be expressed as $\boldsymbol{D} = \varepsilon_0\varepsilon_r(\boldsymbol{E} + \xi\nabla\times\boldsymbol{E})$, $\boldsymbol{B} = \mu_0\mu_r(\boldsymbol{H} + \xi\nabla\times\boldsymbol{H})$, where ξ denotes the chiral parameter which determines the specific rotary power δ through $\delta = -\xi k_0^2 n_0^2$, with k_0 and n_0 representing the wave number in a vacuum and the mean refractive index for a chiral medium, respectively. In this paper, we use δ to measure the strength of chirality. From Maxwell's equations and constitutive relations of chiral medium, the wave equation is derived as

$$\nabla\times\left(\frac{1}{\varepsilon_r}\nabla\times\boldsymbol{H}\right) = k_0^2[\nabla\times(\xi^2\nabla\times\boldsymbol{H}) + \nabla\xi\times\boldsymbol{H} + 2\xi\nabla\times\boldsymbol{H} + \boldsymbol{H}], \quad (1)$$

in which the fields can be expanded into a Fourier series and all the space-dependent electromagnetic parameters should also be expanded in the reciprocal lattice as

$$\boldsymbol{H}(\boldsymbol{r}) = \sum_{\boldsymbol{G}}\boldsymbol{H}(\boldsymbol{G})\,\mathrm{e}^{\mathrm{i}(\boldsymbol{k}+G)\cdot\boldsymbol{r}},$$
$$1/\varepsilon(\boldsymbol{r}) = \sum_{\boldsymbol{G}}\varepsilon^{-1}(\boldsymbol{G})\,\mathrm{e}^{\mathrm{i}\boldsymbol{G}\cdot\boldsymbol{r}},$$
$$\xi(\boldsymbol{r}) = \sum_{\boldsymbol{G}}\xi(\boldsymbol{G})\,\mathrm{e}^{\mathrm{i}\boldsymbol{G}\cdot\boldsymbol{r}},$$
$$\xi^2(\boldsymbol{r}) = \sum_{\boldsymbol{G}}\kappa(\boldsymbol{G})\,\mathrm{e}^{\mathrm{i}\boldsymbol{G}\cdot\boldsymbol{r}}.$$

Then the wave equation for the magnetic field is obtained as

$$\sum_{n=1}^{s}(\varepsilon_{mn}^{-1} - k_0^2\kappa_{mn})[(\boldsymbol{k}+\boldsymbol{G}_n)\times\boldsymbol{H}_n]\times(\boldsymbol{k}+\boldsymbol{G}_m) - \mathrm{i}k_0^2\sum_{n=1}^{s}\xi_{mn})(2\boldsymbol{k}+\boldsymbol{G}_m+\boldsymbol{G}_n)\times\boldsymbol{H}_n = k_0^2\boldsymbol{H}_n, \quad (2)$$

where $\varepsilon_{mn}^{-1} = \varepsilon^{-1}(\boldsymbol{G}_m - \boldsymbol{G}_n)$, $\kappa_{mn} = \kappa(\boldsymbol{G}_m - \boldsymbol{G}_n)$, $\xi_{mn} = \xi(\boldsymbol{G}_m - \boldsymbol{G}_n)$, $\boldsymbol{H}_n = \boldsymbol{H}(\boldsymbol{G}_n)$, $\boldsymbol{H}_m = \boldsymbol{H}(\boldsymbol{G}_m)$, and $k_0^2 = (\omega/c)^2$, and $m,n = 1,2,\ldots,s$ with s being the number of plane waves used in the calculation.

In following simulations, a PhC in a triangular lattice is first investigated. For the convenience of calculation, the relative permittivity of background ε_1, lattice constant a and the diameter $2r$ of holes are chosen to be 4 μm, 2 μm, and 1.7572 μm, respectively. As the scale of chirality, a specific rotary power $\delta_0 = 100^\circ/\mathrm{cm}$ for the chiral background is adopted.

Figure 2(a) shows the band structures of the corresponding chiral PhC for the reference wavelength $\lambda = 1.55$ μm. For comparison, in the three cases the values of specific rotary power in the background δ_1 are set to be 0, δ_0, and $2\delta_0$ respectively, while the value of specific rotary power δ_2 in the holes is set to be 0, i.e., $\delta_2 = 0$ for all the cases.

To describe the polarization distribution, three localized Stokes parameters are used conveniently, among which s_3 can be used to determine whether a polarization state is purely circular ($s_3 = \pm 1$) or purely linear ($s_3 = 0$), s_3 ranges from -1 to 1, whose negative (positive) sign indicates the left-handed (right-handed) polarization state. Figure 2(b) gives the polarization distributions of the first six modes in the chiral PhC, from which one can see that these modes are no longer TE or TM modes, but are elliptical polarization (left-/right-handed EP, LEP/REP) modes generally. For the first four modes, in the center of air holes or part of background, the modes are nearly circular polarized (left-/right-handed CP, LCP/RCP).

For the achiral PhC, the eigen-frequencies of the two paired modes are degenerate at Γ, while for the chiral case, the deviation of the paired modes emerges. The band structure partially zooms in, as shown in the left inset of Fig. 2(a), in which the same type of lines correspond to the same strength of chirality. One can find that after the introduction of chirality, the eigenfrequency bifurcates into two branches; the upper one and the lower one indicate REP and LEP states respectively, and with the increase of chirality, the bifurcation becomes more obvious. This leads to the narrowing of the complete PBG; however, there still maintains a wide PBG corresponding to a central wavelength 1.55 μm. It is concluded that under the condition of weak chirality, the effect of chirality cannot drastically influence the main characteristics of band

structures but trivially modulates the width of a wider PBG; while for a narrow PBG, the effect of chirality becomes relatively significant and may result in the vanishing of the PBG.

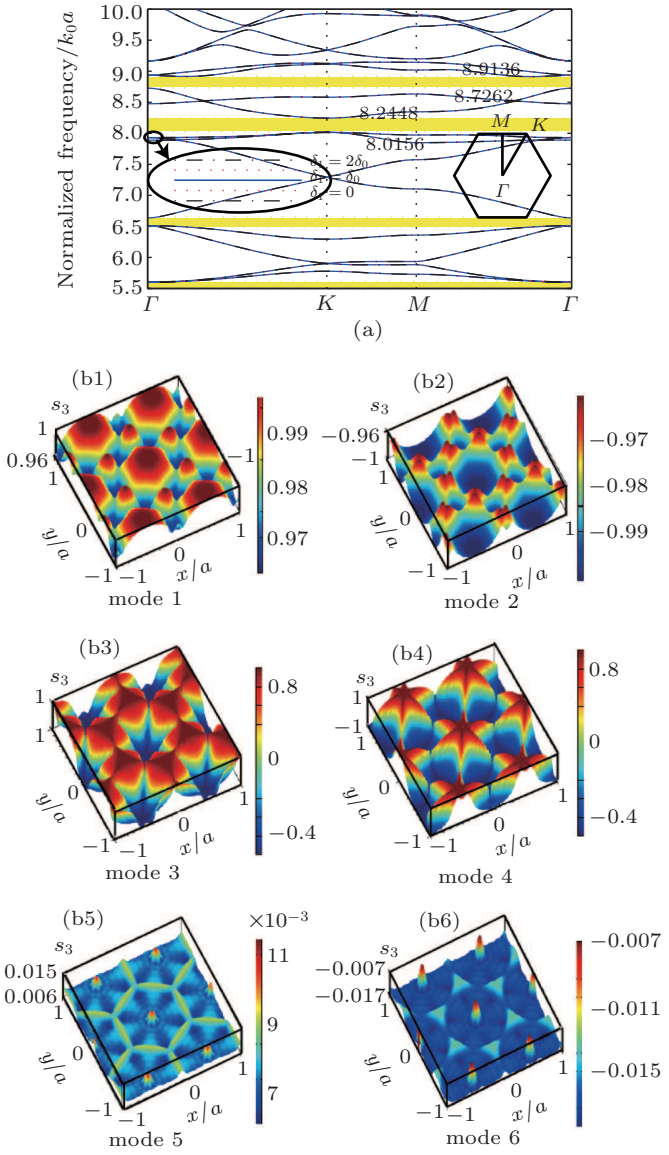


Fig. 2. (color online) Band diagram and polarization distributions for chiral PhC. (a) Band structure versus in-plane wave vector in the irreducible Brillouin zone of the chiral PhC with a triangular lattice, and $\beta a = 8.1073$, the corresponding wavelength $\lambda_0 = 1.55$ μm. (b) Polarization distributions of the first six modes, panels (b1)–(b6) correspond to mode 1, mode 2, . . . , mode 6, respectively.

The wavelength dependences of the mode indices with $\delta_1 = \delta_0$ and $\delta_2 = 0$ are shown in Fig. 3, in which the shaded areas and the dashed line respectively represent the out-of-plane PBGs and air line, and the segment intersected with the shade areas suggests a wavelength range in which guiding light in hollow core is possible. One can find two bands that are suitable for the second and the third optical communication window (near 1.31 μm and 1.55 μm, correspondingly, k_0a from 8.7262 to 8.9136 and from 8.0156 to 8.2448) as indicated in Fig. 2(a).

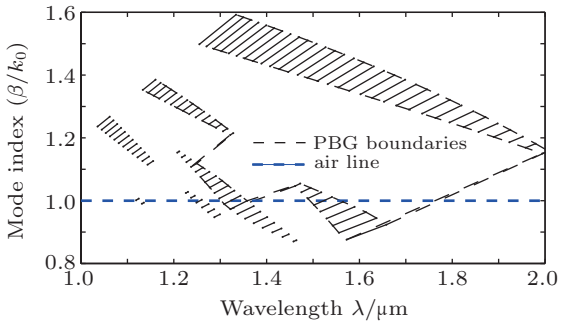


Fig. 3. (color online) Variations of mode indices with wavelength for $\delta_1 = \delta_0$ and $\delta_2 = 0$.

3. Chiral PCF

For a chiral PCF with the same lattice as that of the PhC mentioned above, the modified chiral PWE method[19] is adopted. In the simulation, a 13×13 supercell is used. As indicated in Ref. [19], the circularly polarized state (namely, RCP or LCP) is supported by a chiral PCF with a circular solid core, and the corresponding field distribution is similar to that of achiral PCF. For the chiral PCFs with hollow core, the field distributions of the two fundamental modes are also similar to that for achiral case as depicted in Fig. 4. Figures 4(a) and 4(b) show the field distributions of fundamental modes, where the major semi-axis of the core is parallel to horizontal axis and chosen to be $A = 1.29a$ (hereafter we will choose the lattice constant a as a measure of core size), the minor semi-axis is parallel to perpendicular axis and chosen to be $A = 1.286a$, and the corresponding strength of chirality $\delta_1 = 0$ in Fig. 4(a) (achiral case) and $\delta_1 = 25\delta_0$ in Fig. 4(b) (chiral case), respectively.

The field distributions of guided modes for chiral and achiral cases are alike; however, the corresponding polarization distributions are completely different. Figure 4(c) shows the polarization distributions corresponding to Fig. 4(b) (chiral case), from which one can find that in the area of core both of $|s_3|$ approach to 0.6 which corresponds to elliptical polarization (EP). While for the case of circular hollow core, the corresponding polarized states are almost (circular polarization) (CP) ones. It is clear that the distribution of mode field is mainly dependent on the geometric structure of the PCF under the condition of weak chirality, while the polarization distribution is closely related to the strength of chirality.

To describe the polarization distribution in the core, we redefine the third Stokes parameter for the core as $S_3 = \iint_{S_{\text{core}}} s_3 \left|E^2\right| \mathrm{d}S / \iint_{S_{\text{core}}} \left|E^2\right| \mathrm{d}S$, where $\mathrm{d}S$ denotes the differential area element in the core, and s_3 and $\left|E^2\right|$ represent the corresponding localized third Stokes parameter and intensity of light for $\mathrm{d}S$.

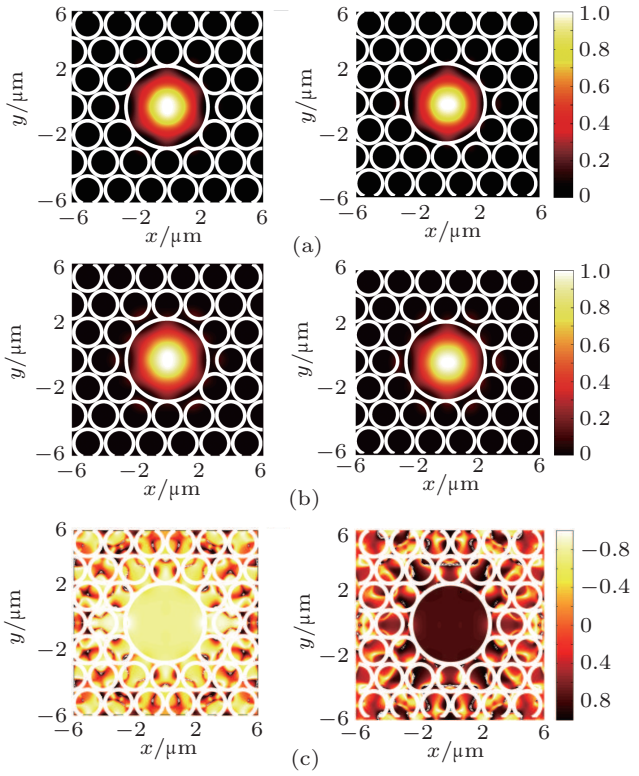


Fig. 4. (color online) The distributions of mode field and corresponding polarization for the first two fundamental modes in chiral PCFs. Panels (a) and (b) show the field distributions of PCFs with the same elliptical hollow core, where the chiralities are chosen to be $\delta_1 = 0$ (achiral case) and $\delta_1 = 25\delta_0$ (chiral case), and the other parameters are the same. Panel (c) shows the polarization distributions corresponding to those in panel (b).

In general, when chiralities in the background and ellipticity both exist in the core, it results in a competition between the linear polarization and circular polarization. In Fig. 5, the effects of chirality and ellipticity on S_3 are compared with each other, where the change in ellipticity of the core is expressed by various values of B with fixed $A = 1.29a$. Figure 5(a) shows the dependences of S_3 on chirality with different values of B, in which the three types of lines correspond to $B = 1.289a$, $B = 1.288a$, and $B = 1.286a$, respectively. Note that the curve of each type of line bifurcates into two branches and the upper and the lower ones represent the right-handed and the left-handed polarization states, respectively.

We define the cases $S_3 \geq 0.99$ and $S_3 \leq -0.99$ as purely RCP and LCP states and the case $|S_3| \leq 0.01$ as linearly polarized state. From Fig. 5(a), one can find that when the chirality nearly vanishes ($\delta_1 \to 0$), all the cases of S_3 degenerate to zero, which indicates that at this time the PCFs support linearly polarized modes. Introducing a small chirality, all $|S_3|$ values fall in a range from 0 to 1, which implies that the EP modes become the ones supported by the PCFs. With the increase of chirality, all $|S_3|$ values almost reach unity, which suggests that the elliptical hollow core PCFs with bigger chirality still support CP modes. This demonstrates that the chirality is dominant in competition with the weak structural asymmetry (ellipticity of core). From the figure, one can also see that the smaller the value of B, the more slowly the $|S_3|$ increases with the rising of δ_1, and for the larger B, it approaches unity faster. For the curve with $B = 1.288a$, a bigger chirality ($\delta_1 \geq 90\delta_0$) is necessary to achieve more purely circular polarization states, while for $B = 1.289a$, the more moderate chirality ($\delta_1 \geq 45\delta_0$) may easily lead to an ideal circular polarization state.

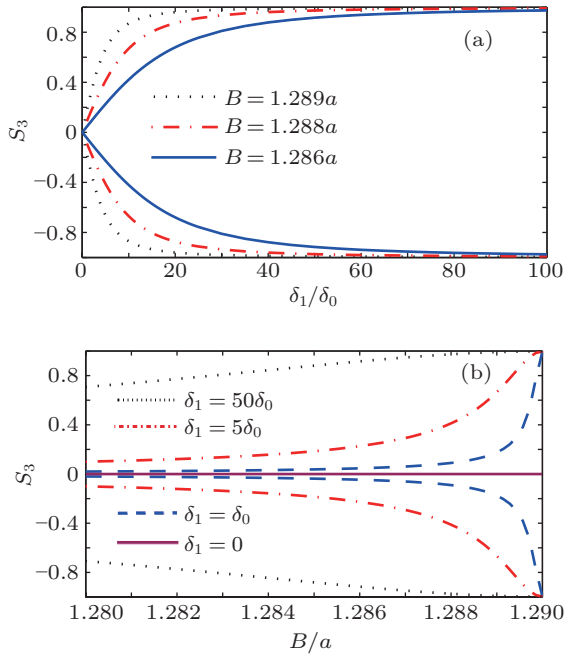


Fig. 5. (color online) The dependence of S_3 on chirality with different B (a) and on ellipticity of the core with different δ_1 (b) for the fundamental modes in chiral PCFs.

The competition is exhibited also by Fig. 5(b), which shows the relationships between S_3 and B with different chiralities and the four types of lines that correspond to $\delta_1 = 0$, δ_0, $5\delta_0$, and $50\delta_0$, respectively. The curve of each type of line bifurcates into two branches except for $\delta_1 = 0$ and the upper and the lower branches also represent right-handed and left-handed polarization states, respectively, which is similar to the case in Fig. 5(a). When $B \leq 1.28a$, all $|S_3|$ values are much smaller than unity; for $\delta_1 = \delta_0$, the modes can be viewed as being linearly polarized. While$B = 1.281a$, $|S_3| \approx 0.1$, which implies that the polarization states can be viewed as EP until $B = 1.29a$. For $\delta_1 = 5\delta_0$, at the very beginning, the polarization states can be viewed as EP up to $B = 1.29a$ due to the interaction of a larger chirality with asymmetry in structure. While for $\delta_1 = 50\delta_0$, the guided modes easily reach CP when $B \geq 1.289a$. But when B approaches to $1.29a$, all $|S_3|$ values are almost equal to unity, which indicates that the chiral PCF with circular core supports CP modes and is independent of the strength of chirality. Therefore, in chiral PCF with an elliptical core, to obtain relatively pure circular polarized modes, a stronger chirality is needed and correspondingly the linear polarization (LP) mode needs a larger core ellipticity.

Figure 6 demonstrates the variations of effective index with chirality for different values of B, in which the lines of

the same type represent the two separate modes: right-handed and left-handed polarization states that the upper and the lower branches correspond to, respectively. The levels of each pair of curves depend on the area of the core. When $\delta_1 = 0$, which corresponds to an achiral case, the separation degree of the initial points ($\delta_1 = 0$) of the curves indicates the strength of LB due to the ellipticity of core. Comparing with the case in Fig. 5(a), the birefringence becomes elliptical birefringence (EB) with the increase of chirality; when the chirality reaches the moderating strength, the birefringence is almost converted into CB. For $B = 1.286a$ corresponding to a stronger structural asymmetry, even if δ_1 approaches to a larger value, say, $20\delta_0$, the chirality hardly affects the effective indices of the pair of modes. With the increase of chirality, the difference between the effective indices emerges gradually. Meanwhile the polarized states are no more LP or CP but EP. For $B = 1.288a$ and $B = 1.289a$, one can see that the effective indices display a smaller LB at first stage corresponding to $\delta_1 \leq 10\delta_0$ and $\delta_1 \leq 5\delta_0$, respectively; when $\delta_1 \geq 90\delta_0$ and $\delta_1 \geq 45\delta_0$, the birefringence becomes CB. It is concluded that at the beginning, the structural asymmetry is dominant, which corresponds to LB, with the increase of chirality, the effect of chirality becomes stronger and even superior to that of structural asymmetry, which makes CB dominant.

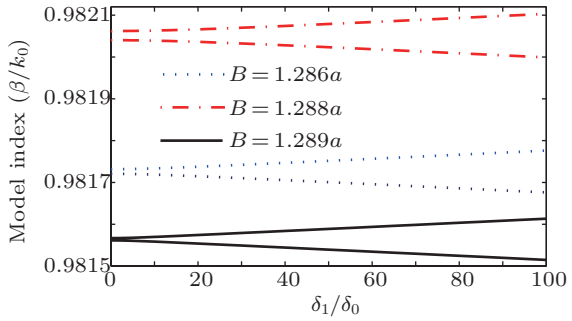


Fig. 6. (color online) Effective indices of fundamental modes in chiral PCFs, where $\lambda_0 = 1.55$ μm.

4. Conclusions

In this paper, we investigate a kind of dielectric-chiral PCF with an elliptical hollow core. Owing to the chirality of the background and the ellipticity of the core, the PCFs support complicated polarized modes, from the LP one to CP one operating in an optical fiber communication band. In an elliptical hollow core PCF, when the chirality is relatively weak, the polarized states are almost LP and will become EP with the increase of chirality, when the chirality reaches an appropriate strength, the modes are almost converted into CP.

For a chiral PCF with a circular hollow core, the polarized states are CP and are independent of the strength of chirality. The stronger the chirality, the larger the CB will be. The moderate chirality is necessary to obtain the more purely CP states or the larger birefringence for a PCF with asymmetric core. These unique properties are promising for applications in optical fiber communication, such as the circularly or elliptically polarized filter, elliptical polarization maintaining PCF, and lasers.

References

[1] Knight J C, Birks T A, Russell P S and Atkin D M 1996 *Opt. Lett.* **21** 1547
[2] Birks T A, Knight J C and Russell P S 1997 *Opt. Lett.* **22** 961
[3] Liu S and Li S G 2013 *Chin. Phys. B* **22** 074206
[4] Reeves W H, Skryabin D V, Biancalana F, Knight J C, Russell P S J, Omenetto F G, Efimov A and Taylor A J 2003 *Nature* **424** 511
[5] Zhang Y N 2012 *Acta Phys. Sin.* **61** 084213 (in Chinese)
[6] Yan H F, Yu C Y, Tian H D, Liu Y M and Han L H 2010 *Acta Phys. Sin.* **59** 3273 (in Chinese)
[7] Zhang X J, Zhang J L and Hou J P 2007 *Acta Phys. Sin.* **56** 4668 (in Chinese)
[8] Yan F P, Li Y F, Wang L, Gong T R, Liu P, Liu Y, Tao P L, Qu M X and Jian S S 2008 *Acta Phys. Sin.* **57** 5735 (in Chinese)
[9] Liu S, Li S G, Yin G B and Wang X Y 2012 *Chin. Phys. B* **21** 034217
[10] Barkou S E, Broeng J and Bjarklev A 1999 *Opt. Lett.* **24** 46
[11] Cregan R F, Mangan B J, Knight J C, Birks T A, Russell P S J, Roberts P J and Allan D C 1999 *Science* **285** 1537
[12] Wang W, Hou L T, Song J J and Zhou G Y 2009 *Chin. Phys. Lett.* **26** 054204
[13] Zhao X T, Liu X X, Zheng Y, Han Y, Zhou G Y, Li S G and Hou L T 2012 *Acta Phys. Sin.* **61** 214210 (in Chinese)
[14] Xiao L M, Jin W, Demokan M S, Ho H L, Tam H Y and Ju J 2006 *Opt. Lett.* **31** 1791
[15] Wang H L, Yang A J and Leng Y X 2013 *Chin. Phys. B* **22** 074208
[16] Steel M J and Osgood R M 2001 *Opt. Lett.* **26** 229
[17] He Z J 2009 *Chin. Opt. Lett.* **7** 387
[18] Du Y, Li S G and Liu S 2012 *Chin. Phys. B* **21** 094219
[19] Li J Q, Su Q Y and Cao Y S 2010 *Opt. Lett.* **35** 2720
[20] Wong G K L, Kang M S, Lee H W, Biancalana F, Conti C, Weiss T and Russell P S J 2012 *Science* **337** 446
[21] Kopp V I and Genack A Z 2011 *Nat. Photonics* **5** 470
[22] Liu H T, Wei Y Y, Gong Y B, Yue L N and Wang W X 2006 *Chin. Phys.* **15** 2114
[23] Zhao C J, Fan D Y, Peng R W and Tang Z X 2006 *Chin. Phys. Lett.* **23** 2793
[24] Kopp V, Churikov V M, Singer J, Chao N, Neugroschl D and Genack A Z 2004 *Science* **305** 74
[25] Shemuly D, Ruff Z M, Stolyarov A M, Spektor G, Johnson S G, Fink Y and Shapira O 2013 *Opt. Express* **21** 1465
[26] Li J Q, Li S, Wang X O, Zheng Y D and Li C F 2004 *Chin. Phys. Lett.* **21** 475
[27] Cao Y S, Li J Q and Su Q Y 2011 *J. Opt. Soc. Am. B* **28** 319
[28] Jin L, Li J Q, Li H M, Lin Q F and Li C F 2007 *Opt. Commun.* **279** 43
[29] He C, Lu M H, Yin R C, Fan T and Chen Y F 2010 *Appl. Phys.* **108** 073103
[30] Arismar C S, Lona D G, Oliveira I D, Figueroa H E H and Fragnito H L 2011 *Opt. Lett.* **36** 133